

UCSF

UC San Francisco Electronic Theses and Dissertations

Title

Kinetic Proofreading In T Cell Activation Is Distributed Across Multiple Membrane Proximal Signaling Complexes

Permalink

<https://escholarship.org/uc/item/8q71q03z>

Author

Britain, Derek Michael

Publication Date

2021

Peer reviewed|Thesis/dissertation

Kinetic Proofreading In T Cell Activation Is Distributed Across Multiple Membrane Proximal Signaling Complexes

by
Derek Britain

DISSERTATION
Submitted in partial satisfaction of the requirements for degree of
DOCTOR OF PHILOSOPHY

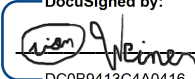
in

Biophysics

in the

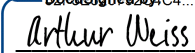
GRADUATE DIVISION
of the
UNIVERSITY OF CALIFORNIA, SAN FRANCISCO

Approved:

DocuSigned by:

DC0B9413C4A0416... Orion Weiner
Chair

DocuSigned by:

Hana El-Samad

DocuSigned by:

A45915AB27B74F5... Arthur Weiss

Committee Members

Copyright 2021

By

Derek Britain

For Shohini.

My wife and best friend.

Acknowledgements

Nothing exists quite like the experience of graduate schooling. I expected create a project, run some experiments, analyze some data, and publish my work. While all these things happen, graduate school is so much more. You don't realize you are essentially running a start-up company of one that grows to define you as you pour in all your energy, resources, and self-worth. The successes are intoxicating and the failures often devastating. Unfortunately the failures occur much more often than the successes. Somehow we make it through but certainly not alone. I have many to thank for helping me weather the storms and remind me to celebrate even the smallest of victories.

I would like to thank my advisor Orion, for being a constant source of optimism, ideas, and support, both in- and out-side of the lab. Through multiple project failures and pivots, Orion never imparted a discouraging word or thought, and instead always reassured me a path forward existed. Orion's never ending optimism and excitement for science defy understanding. More importantly Orion genuinely cares about everyone of his mentees as a person. When life challenged me with a long-distance marriage for a year and a half, Orion never once mentioned the time I took to travel or my suffering productivity, and instead offered any help he could give. Without Orion's unwavering support, I doubt I would be writing this dissertation.

My thesis committee, Art Weiss and Hana El-Samad, offered continual encouragement, ideas, and support over the years. Art is the genius, gentleman, godfather of T cell signaling. His knowledge, intuition, and input were a privilege to have throughout my

thesis project. Hana provided me much needed grounding and pragmatism throughout my thesis. Also I'll always be grateful for her handling of my qualifying exam when one of my committee members failed to appear.

Many current and former members made my thesis lab an enjoyable and supportive environment over the years. Thank you Jeff Alexander for being a fantastic rotation mentor and an all around great person. Thank you Kirsten Meyer for your input and reassurance as I distracted you almost daily with brainstorming, venting, and general ranting. Thank you Doug Tischer for giving me a crash course in T cell signaling, protein biochemistry, surface modification, lipid chemistry, and for producing the abundance of reagents I used daily in my thesis. Thank you Anne Pipathsouk, Rachel Burunetti, Tamas Nagy, and Jason Town for being with me day-in and day-out in the lab.

To my undergraduate research advisor, Roger Brent, and labmates, Alex Mendenhall and Bryan Sands, thank you for reigniting my passion for scientific research and encouraging me to pursue a doctorate.

Thank you to my family for always being supportive and expressing interest even if they did not understand what I was doing, and many friends, old and new, who kept me grounded and reminded me life existed outside of graduate school.

Finally I'd like to thank my wife and best friend Shohini for being by my side through all of the ups and downs of graduate school. I could not imagine doing this without you.

Statement Regarding Author Contributions

The following will become a manuscript draft intended for publication:

Derek Britain, Orion D. Weiner. Kinetic Proofreading In T Cell Activation Is Distributed Across Multiple Membrane Proximal Signaling Complexes. I conceived, designed, and performed all experiments, and wrote the manuscript under the guidance of Orion Weiner. I utilized and adapted protocols, plasmids, and purified proteins produced by Doug Tischer previously in the lab. Orion Weiner, Arthur Weiss, and Hana El-Samad offered input and guidance throughout the project.

Abstract

Kinetic Proofreading In T Cell Activation Is Distributed Across Multiple Membrane Proximal Signaling Complexes

Derek Britain

T cells measure the lifetime of antigen binding events to discriminate self from foreign antigens. The full mechanism behind this kinetic proofreading behavior remains elusive. Previously, we developed a light-gated immune receptor to directly test the kinetic proofreading model in T cell antigen signaling. We found evidence of a kinetic proofreading mechanism upstream of the generation of the signaling lipid diacylglycerol (DAG). Here, we modify our assay to be compatible with more live-cell biosensors, and measure the magnitude of kinetic proofreading behavior at multiple upstream events in T cell antigen signaling. We found that kinetic proofreading behavior exists in receptor activation, with greater proofreading at the formation of LAT clusters, and even greater proofreading at the generation of DAG. These data suggest that the mechanism of proofreading is distributed among receptor activation, LAT cluster formation, and DAG generation from fully mature LAT clusters. Having kinetic proofreading steps beyond the individual receptor creates the possibility of cooperativity between multiple active receptors for antigen discrimination.

Table of Contents

INTRODUCTION	1
RESULTS	4
DISCUSSION	9
CONCLUSION	14
METHODOLOGY	15
REFERENCES	25

List of Figures

FIGURE 1	36
FIGURE 2	37
FIGURE 3	37
FIGURE 4	39
FIGURE 5	40
FIGURE S1	41
FIGURE S2	42
FIGURE S3	43

Introduction

Proper antigen discrimination is a cornerstone of the adaptive immune system. Failure of T cells to activate in response to foreign antigen potentially enables pathogens to invade the body undetected. Conversely, improper T cell activation against self-antigen causes autoimmune disorders. When a T cell contacts an antigen-presenting cell (APC), it can detect the presence of 1-10 molecules of foreign-antigen (Christinck et al., 1991; Demotz et al., 1990; Kimachi et al., 1997; Sykulev et al., 1996), despite the much greater abundance (100,000x or more) of self-antigen (Bhardwaj et al., 1993; Cohen et al., 2003; Irvine et al., 2002; Unternaehrer et al., 2007). Simple changes in receptor occupancy cannot explain T cell sensitivity to foreign-antigen (Daniels et al., 2006; M. M. Davis et al., 1998; Gascoigne et al., 2001; Germain & Stefanová, 1999).

One popular model for how T cells discriminate antigen is the kinetic proofreading model (McKeithan, 1995; Ninio, 1975), where only antigens that continuously bind a TCR for a threshold duration activate the T cell (**Fig 1A**). Kinetic proofreading postulates that antigen binding begins a series of irreversible events that must progress to completion before activating the T cell. If the antigen unbinds the TCR before all events are complete, the system resets back to the ground state. Only antigen that stays bound to the TCR long enough for the completion of all events is stimulatory to the T cell. This allows T cells to ignore numerous short-lived self-antigen binding events, while activating in response to long-lived foreign-antigen binding events (M. M. Davis et al., 1998; Gascoigne et al., 2001; Germain & Stefanová, 1999).

Kinetic proofreading mechanisms are utilized in a number of cellular processes, giving DNA replication, protein translation, and mRNA splicing specificity far beyond what binding affinities predict alone (Burgess & Guthrie, 1993; Hopfield, 1974; Ninio, 1975). While it is commonly accepted that T cells use kinetic proofreading for antigen discrimination (Coombs & Goldstein, 2005; McKeithan, 1995), we do not know what events in antigen signal transduction constitute the series of irreversible events.

Previously, our group developed and used a light-gated immune receptor to measure kinetic proofreading in T cell antigen signal transduction. We found proofreading behavior upstream of DAG generation, while seeing no proofreading behavior in the recruitment of Zap-70 to the activated receptor (**Fig 1B**) (Tischer & Weiner, 2019). This suggested that kinetic proofreading steps exist between Zap70 recruitment to bound receptors, and DAG generation.

Here we improve our assay by incorporating the native integrin ICAM-1, which improves the robustness of our previous biosensors and enables the use of new biosensors (**Fig 2A**) (Bromley & Dustin, 2002). With integrin adhesion, we now measure kinetic proofreading in receptor activation upstream of the recruitment of Zap-70. We measure stronger upstream kinetic proofreading at the clustering of the scaffold protein LAT, suggesting proofreading steps between Zap-70 recruitment and LAT cluster formation. Furthermore, we measure the strongest upstream kinetic proofreading at DAG generation, suggesting additional proofreading steps after the initial formation of LAT clusters. We also find that LAT clusters reset slower than Zap-70 recruitment upon

unbinding antigen. Our results suggest a kinetic proofreading system that starts with receptor activation and continues across multiple spatially segregated signaling intermediates, with terminal signaling intermediates resetting slower than initial signaling intermediates. Such a system would allow high concentration of antigens with intermediate binding life-times to activate T cells while still responding to rare long-binding antigens and filtering out short-binding antigens(Cameron et al., 2013; Goyette et al., 2020; Korem Kohanim et al., 2020; Lin et al., 2019; Pettmann et al., 2021; Wang et al., 2020).

Results

ICAM-1 adhesion enables robust reporter dynamics

To further dissect kinetic proofreading in antigen signal transduction we required an adhesion system that enabled robust biosensor dynamics while maintaining a sufficient cell footprint for live-cell tracking. We functionalized our functionalized supported lipid bilayers (SLB) with human ICAM-1 to better mimic the T cell / APC interaction (**Fig 2A**) (Dustin et al., 2007). We reformulated our SLBs to include 1% mol DGS-NTA(Ni) lipids for attaching poly-his-tagged ICAM-1 (ICAM-1-His), while keeping 1% mol biotinyl-cap PE lipids for attaching biotinylated LOV2 via Streptavidin (Nye & Groves, 2008). We first validated Zap70 recruitment, LAT clustering, and DAG generation biosensors expressed in Jurkat cells on ICAM-1 functionalized bilayers (**Fig 2B**). Jurkat cells stably expressing Zdk-CAR were exposed to SLBs functionalized with purified ICAM-1-His and alexa fluor 488 labeled LOV2 (LOV2-AF488). To increase integrin binding, we modified our imaging buffer to a modified HBSS (mHBSS) buffer with Ca^{++}/Mg^{++} (Labadia et al., 1998). Compared to our previous antibody based adhesion, Jurkats on ICAM-1-His functionalized bilayers released a greater percentage of the bound AF488-LOV2 ligand upon blue-light illumination (**Fig 2C**). Adhesion through ICAM-1-HIS increased the dynamic range of the DAG biosensor, Zap70 recruitment biosensor, and LAT clustering biosensor while also showing more native recruitment patterns (**Fig 2B**) (Balagopalan et al., 2015; Chakraborty & Weiss, 2014).

Quantifying kinetic proofreading in Zap70 recruitment, LAT clustering, and DAG generation.

To quantify the magnitude of kinetic proofreading behavior at a signaling step, we ask if ligand receptor occupancy or ligand binding half-life best explain the signaling step's output (Tischer & Weiner, 2019). We measure a cell's receptor occupancy and signaling output by subjecting the Zdk-CAR to an intensity of blue light with a known ligand binding half-life until a steady-state is reached. After three minutes of illumination when a steady state is reached, we image the amount of bound LOV2-AF488 accumulated underneath every cell using a long exposure image (O'Donoghue et al., 2013), and the output intensity of the signaling biosensor (**Fig 3A**). We then reset the system with a two minute pulse of intense blue-light to stop all signaling, before illuminated the cells with the next intensity of blue light. We repeat the experiment on bilayers functionalized with different densities of LOV2-AF488 to sample a wider range of occupancies. Following this experimental protocol, we build up a dataset of signaling output as a function of both ligand occupancy and ligand half-life.

Next we fit our data to a simple model of the expected output from a kinetic proofreading signaling system (**Fig 3B**). In the model, signaling output is a function of receptor occupancy (**R**) multiplied by ligand binding half-life (τ) raised to the number of strong proofreading steps (**n**). While certain assumption of the model, such as equivalent strength of all proofreading steps, make the fit value of **n** unlikely to represent the actual number of upstream proofreading steps, we can compare the

relative value of n of a signaling step to other steps in the cascade to understand how proofreading behavior changes as we progress through the signaling system.

Receptor activation and Zap70 recruitment show moderate kinetic proofreading

Using the ICAM-1-His functionalized bilayers, we measure moderate amounts of kinetic proofreading behavior in the recruitment of Zap70 to activated receptors. Zap70 recruitment correlated with both receptor occupancy ($\rho = 0.41$) and ligand binding half-life ($\rho = 0.49$) (**Fig 4A**). Our model fit an average of 4.5 proofreading steps across three datasets ($n = 4.5 \pm 0.4$) (**Fig 4B,C**). These data suggest the existence of kinetic proofreading steps between LOV2 binding and Zap70 recruitment.

In our previous work, we measured no kinetic proofreading in Zap70 recruitment. Before we measured Zap70 with no adhesion to the bilayer as antibody adhesion inhibited Zap70 reporter dynamics. With no additional adhesion, only actively signaling cells adhere to the bilayer. In those conditions we potentially missed sampling high occupancy, short half-life regimes with little Zap70 recruitment, as those cells failed to adhere to the bilayer. If we filter out the short half-life conditions of our new Zap70 data and refit our kinetic proofreading model, we achieve a similarly low proofreading result ($n=0.7 \pm 0.3$) (**Fig S1**).

LAT clustering and DAG generation show increasing proofreading behavior

Next we measured the strength of proofreading behavior beyond the receptor, at the clustering of LAT and at the generation of DAG. LAT clustering showed an increased

dependency on binding half-life ($\rho=0.54$) and a decreased dependence on receptor occupancy ($\rho=0.21$) compared to Zap-70 recruitment (**Fig 4A**). Our proofreading model best fits our LAT data with about 8 steps of proofreading ($n=7.8\pm 1.1$) (**Fig 4B,C**). We measured stronger kinetic proofreading behavior in LAT clustering than Zap70 recruitment, suggesting additional steps of kinetic proofreading between the recruitment of Zap-70 to phosphorylated ITAMs and the formation of LAT clusters. The generation of DAG also depended heavily on ligand half-life ($\rho=0.52$), while depending the least on occupancy ($\rho=0.18$). Our model fits the highest number of kinetic proofreading steps at DAG generation ($n=11.3 \pm 1.5$), suggesting further kinetic proofreading steps beyond initial LAT clustering until the generation of DAG and release of IP3. The simulated output of a kinetic proofreading system with the same number of proofreading steps that we measured in each biosensor matched our experimental data well (**Fig 4D**).

LAT clusters reset more slowly than Zap70 clusters upon ligand disengagement

Our Zdk-CAR deactivates with blue light, giving us the unique ability to unbind all antigen binding events synchronously. After measuring additional kinetic proofreading steps downstream of the activated receptor, we used our Zdk-CAR system to measure the off-rate of recruited Zap-70 and clustered LAT upon acute antigen unbinding (**Fig 5A**). After allowing cells to activate on LOV-AF488 and ICAM-1-HIS functionalized bilayers for three minutes, we acutely unbound all LOV2 ligand with intense blue light while imaging LOV2, Zap70 and/or LAT biosensors . We segmented individual sub-

cellular clusters of each respective biosensor, and fit their off-rate curves with bi-exponential functions (**Fig 5B**).

We found that clusters of receptor-bound LOV2 dissociated with an average half-life of 6.6 seconds. Clustered Zap70 dissociated on a similar timescale, with an average dissociation half-life of 7.8 seconds. Meanwhile LAT clusters dissociated much slower than LOV2 ligand or Zap70, with an average half-life of 18.8 seconds. Upon ligand unbinding, the receptor and LAT signaling complexes dissociate with different off rates. This opens the possibility that a LAT cluster could survive a momentary ligand unbinding event, and integrate multiple ligand binding events (Lin et al., 2019).

Discussion

Kinetic proofreading enables T cells to discriminate self- from cognate-antigens by measuring antigen binding half-life. However, the kinetic proofreading mechanism underlying antigen discrimination is not fully understood. Using our Zdk-CAR system, we measured the dependency of Zap70 recruitment, LAT clustering, and DAG generation on antigen binding half-life and receptor occupancy. We found evidence for kinetic proofreading behavior in antigen signal transduction as early as Zap70 recruitment to phosphorylated receptor ITAMs. We measured greater kinetic proofreading behavior at the clustering of the scaffold protein LAT, and the most kinetic proofreading behavior at the generation of the signaling lipid DAG. Our findings suggest that the mechanism of kinetic proofreading underlying T cell antigen discrimination spans multiple membrane associated signaling complexes (Yi et al., 2019).

After a receptor binds an antigen, many events must occur before Zap70 is recruited to the receptor's ITAMs. While we cannot assign importance or strength to any single potential proofreading step, many strong candidates exist (Chakraborty & Weiss, 2014). The binding event excludes the bulky phosphatase CD45 that would otherwise rapidly dephosphorylate the ITAMs (S. J. Davis & van der Merwe, 2006; Springer, 1990). The receptor itself could undergo mechanical conformational changes making it more accessible for phosphorylation (Kim et al., 2009, 2010). An active molecule of the src-family-kinase Lck must phosphorylate the receptor (Schoenborn et al., 2011; Tan et al., 2014). Finally, Zap70 must overcome autoinhibition before binding the phosphorylated receptor with both of its tandem SH2 domains (Deindl et al., 2009, 2009; Hsu et al.,

2017). Additional proofreading steps may exist that are not captured in our system such as CD4/8 coreceptor scanning (Stepanek et al., 2014) and CD3 ζ ITAM allostery (Borroto et al., 2014). Others have also suggested receptor level proofreading through measuring a temporal delay between receptor binding and Zap70 recruitment for both TCRs (Huse et al., 2007; Yi et al., 2019), and CARs (Bhatia et al., 2005).

We measured stronger proofreading behavior downstream of Zap70 recruitment at the clustering of LAT and the generation of DAG. This result implies that additional kinetic proofreading steps exist separate from the receptor. The additional proofreading steps measured at LAT clustering could be the full activation of Zap70 through phosphorylation, and/or the many phosphorylation and binding events on LAT required to initiate clustering. Hyperactive Zap70 mutants biased towards the active conformation increase T cell response to normally weak agonists, suggesting that pre-activation Zap70 short-circuits a proofreading step(s) (Shen et al., 2021).

The further proofreading measured in DAG generation suggests additional steps beyond the initial clustering of LAT. LAT does not require the phosphorylation of all its tyrosines, or binding of all known associated proteins, to cluster (Su et al., 2016). These further phosphorylation and protein recruitment events may be required for a LAT cluster to mature into a fully signaling competent complex. A strong candidate for an additional proofreading step is phosphorylation of LAT Y132. Y132 is an evolutionarily conserved poor substrate for its kinase Zap70, and is required for PLC ζ recruitment, DAG generation, and Ca⁺⁺ mobilization (Andreotti et al., 2010; Courtney et al., 2018).

Mutation of this site to a better Zap70 substrate which rapidly phosphorylates resulted in increased T cell activation to normally weak agonists (Lo et al., 2019). Furthermore, Sherman et al. found that PLC β is recruited to only a subset of LAT clusters, suggesting that only a subset of LAT clusters reach a fully signaling competent state (Sherman et al., 2011).

We measured kinetic proofreading strength from ligand binding to DAG generation. It is possible additional and/or different kinetic proofreading steps exist in other branches of the T cell antigen signal transduction system. Recently Huang et al. measured a kinetic lag between the recruitment of SOS to LAT clusters and its full activation, which they attributed to allosteric rearrangements within SOS itself (Huang et al., 2019).

The kinetic proofreading model requires all intermediate steps to reset upon unbinding of the ligand (**Fig 1A**). This means that information about the receptor's binding state must be communicated to all proofreading steps. If kinetic proofreading steps exist beyond the T cell receptor, how is unbinding information propagated beyond the receptor? An attractive mechanism is the segregation of CD45 away from bound receptors, creating spatial regions in which activating events can occur (S. J. Davis & van der Merwe, 2006). Superresolution microscopy by Razvag et al. measured TCR/CD45 segregated regions within seconds of antigen contact at the tips of T cell microvilli (Razvag et al., 2018). Upon unbinding these regions collapse and CD45 dephosphorylates receptor ITAMs and LAT clusters.

What are the advantages of distributing kinetic proofreading beyond the receptor?

Having subsequent proofreading steps separate from the receptor allows cooperativity between multiple receptors in activating downstream signaling steps (e.g. multiple activated receptors contributing to the creation and maturation of a single LAT cluster). Larger TCR cluster size increases the probability of T cell activation (Manz et al., 2011). Lin et al. observed cooperativity between single TCR/pMHC binding events, where shorter binding events that overlapped in space and time activated NFAT translocation similar to long-lived single binding events in primary murine T cells (Lin et al., 2019).

Kinetic proofreading beyond single receptors with cooperativity could explain T cell activation in response to lower affinity self- and tumour antigens (Yin et al., 2012). An antigen binding long enough to activate a single receptor but not long enough to satisfy downstream proofreading steps could still activate a T cell if it cooperated with other active receptors to satisfy those steps. Such a mechanism has been implied in autoimmunity (Korem Kohanim et al., 2020; Wang et al., 2020), and immunotherapy off target effects (Cameron et al., 2013).

Work on kinetic proofreading often assumes that the reset rate after ligand binding is uniform across all signaling intermediates (**Fig 1A**). However, in his seminal work applying the mathematical framework of kinetic proofreading to TCR activation, Timothy McKeithan postulated that a kinetic proofreading system with slower reset rates for downstream events compared to upstream signaling events would respond to true cognate-antigen binding events a higher percentage of the time while still ignoring weak

self-antigen binding events (McKeithan, 1995). Recently, Pettman et al. modeled how slower resetting of terminal signaling complexes could account for fraction steps in their measurements of the number of proofreading steps (Pettmann et al., 2021). We measured slower dissociation of downstream LAT clusters compared to the upstream events of ligand binding and Zap-70 recruitment (**Fig 5**). Our data suggests a LAT cluster could survive an unbinding event that deactivates an active receptor, and be matured to a full signaling entity by multiple shorter binding events.

If CD45 dephosphorylates both receptor ITAMs and LAT, why do the off rates of Zap-70 and clustered LAT differ? A potential mechanism explaining this difference is how the proteins making up each respective protein cluster bind their phosphorylated substrates. A bound protein protects the bound phospho-tyrosine from dephosphorylation. Goyette et al theorize that Zap-70 kinetically binds phosphorylated ITAMs, oscillating binding the ITAMs between its two SH2 domains (Goyette et al., 2020). This leaves the phosphorylated ITAMs open to dephosphorylation by CD45. Alternatively, the proteins binding phospho-tyrosine in LAT clusters could be statically bound, where the CD45 dephosphorylation rate would be limited to the inherent unbinding rate of proteins in the cluster. Alternatively, LAT clusters exclude CD45, potentially limiting dephosphorylation to the periphery of the cluster (Su et al., 2016).

Conclusion

Kinetic Proofreading exists in activation of the T cell receptor, yet the magnitude of kinetic proofreading behavior increases beyond the activated T cell receptor. This suggests kinetic proofreading steps exist beyond individual TCRs. Furthermore, signaling steps downstream of the receptor reset slower than the receptor itself upon ligand unbinding. Kinetic proofreading steps beyond an individual receptor that reset at a slower rate enable T cells to respond to antigens with intermediate binding half-lives when presented in sufficiently high concentrations, while still responding to single long-lived antigen binding events.

Methodology

Methods were adapted from our lab's previous work (Tischer & Weiner, 2019) with modified sections highlighted below.

Cloning

We used standard molecular biology protocols for all cloning. In general, We PCR amplified individual DNA segments and assembled them using the isothermal Gibson assembly method. Mark M Davis (Huse et al., 2007) kindly gifted us a plasmid encoding the C1 domains of PKC θ . Jay Groves kindly gifted us plasmids encoding Zap70 and LAT (O'Donoghue et al., 2013). The Zdk-CAR was based on a CD8-CAR (Irving & Weiss, 1991), the plasmid for which was a kind gift from Art Weiss. The V529N mutation in LOV2 biases it towards the 'open' conformation which does not bind Zdk (Yao et al., 2008). This mutation facilitated the quick release of LOV2 from the Zdk-CAR.

Cell culture

Jurkat cells grew in RPMI 1640 (Corning Cellgro, #10-041-CV) supplemented with 10% fetal bovine serum (Gibco, #16140-071) and glutamine (Gibco, #35050-061). We maintained Jurkats at densities between 0.1 and 1.0 $\times 10^6$ cells per ml. We grew 293 T cells in DMEM (Gibco, #11995-065) with 10% fetal bovine serum. All cell lines grew in humidified incubators at 37°C with 5% CO₂.

Cell line construction

We combined 1 ml of wt Jurkat cells at 0.5×10^6 cells/ml with 0.5 ml lentiviral supernatant for the Zdk1-CAR and the appropriate reporter construct. Cells recovered overnight in the incubator, 8 ml of media was added the following day and cells were grown to desired density. Cells were labeled with the Halo dye JF549 (Grimm et al., 2015) and we sorted the desired expression levels by FACS (FACSAria II, BD). Cells recovered for approximately three passages and tested for blue-light dependent signaling on LOV2 and ICAM-1 functionalized SLBs on the microscope. We obtained wild-type Jurkat cells for this study from the laboratory of Dr. Art Weiss. Regular mycoplasma tests were negative.

Lentiviral production

We produced lentivirus in 293 T cells using a second-generation lentiviral system (James & Vale, 2012). We transfected Cells grown to 40–60% confluency in 6-well plates with 0.5 ug each of pHR (containing the transgene of interest), pMD2.G (encoding essential packaging genes) and p8.91 (encoding VSV-G gene to pseudotype virus) using 6 ul of Trans-IT (Mirus, #MIR 2705) per manufacturer's instructions. (Plasmids kind gift from Ron Vale.) After 48 hr, we filtered the supernatant through a 0.22 um filter and used immediately or froze at -80°C until use.

Cell preparation for imaging

For each imaging well, we used approximately 1×10^6 Jurkat cells labeled with the Halo dye JF549 (Grimm et al., 2015) (10 nM, a kind gift from the Lavis lab) for at least 15 min at 37°C before resuspension in growth media. Before imaging, we washed cells once into mHBSS-BB (at 400 RCF, 4 min), resuspended them in 40 ul imaging media before adding them to a functionalized SLB.

Protein purification

LOV2 and Zdk were purified and labeled as previously described in our previous work (Tischer & Weiner, 2019). Jay Groves generously gifted us the purified human ICAM-1-HIS used in this study (Nye & Groves, 2008).

Glassware cleaning

All glassware was cleaned as described in our previous work (Tischer & Weiner, 2019).

Preparation of small unilamellar vesicles (SUVs)

We washed a precleaned 4 ml glass vial 2x with chloroform (Electron Microscopy Sciences, #12550). Using Hamilton syringes (Hamilton Company, Gastight 1700 series, #80265 and #81165), we combined 1 mmoles of lipids in the following molar ratio: 97.5% DOPC, 0.5% PEG-PE, 1% DGS-NTA(Ni) and 1% biotinyl CAP PE (Avanti Polar Lipids, #850375C, #880230C, #790404C, #870282C, respectively). Next we evaporated the chloroform by slowly rotating the vial at an angle while slowly flowing nitrogen gas (Airgas, #NI 250). We vacuum desiccated the resulting lipid film for 2 hours or overnight.

After desiccation, We rehydrated the lipids in 2ml of TBS and gently vortexed the vial for 10 min. We transferred the mixture to a cleaned 5 ml round bottom glass tube. We formed SUVs by submerging bottom of the tube in a Branson 1800 ultrasonic cleaner (Branson #M1800) to the level of the lipid mixture in the tube and sonicating for 30-60 minutes until clear. We added ice periodically to the sonicator bath to maintain temperature. Centrifugation at >21,000 RCF for 30 min at 4C (Eppendorf microcentrifuges 5425R) pelleted large lipid structures. We removed the SUV containing supernatant and stored it in liquid nitrogen until use.

RCA cleaning of microscopy coverslips

We placed Glass coverslips (Ibidi, #10812) into a glass Coplin jar (Sigma-Aldrich, #BR472800) and successively bath sonicated for 10 min each in acetone (Sigma-Aldrich, #534064-4L), isopropyl alcohol (Fischer, #BP2618500), and ddH₂O. Coverslips were washed five times in ddH₂O between each bath sonication to remove excess organic solvents. Next we added 40 ml ddH₂O, 10ml of 30% ammonium hydroxide, and 10 ml 30% hydrogen to the coverslips. We placed the Coplin jar into a 70–80°C water bath and allowed it to react for 10 min after the base solution began to vigorously bubble . We decanted the base solution and washed the coverslips five times in ddH₂O. Next, we added 40ml ddH₂O, 10ml of 30% hydrochloric acid, and 10ml 30% hydrogen peroxide to the coverslips. Again we incubated the reaction in the water bath and allowed it to react for 10 minutes after the acid solution began to vigorously bubble. We decanted the acid solution and washed the coverslips five times in ddH₂O and stored them in ddH₂O for up to one week.

Functionalization of SLBs and cell preparation

After removing an RCA cleaned glass coverslip from ddH₂O and immediately blown drying it with compressed nitrogen, we firmly attached a six-well Ibidi sticky chamber (Ibidi, #80608) to the coverslip. We diluted 30 ul of SUV mixture with 600 ul TBS before adding 100ul to each well and incubated at room temperature for 25 minutes. To functionalize a well, we flushed out excess lipids with 500 ul TBS. Next we added 100ul of ICAM-1-HIS diluted in TBS-BB to 150uM to the well and incubated at room temperature for 35 minutes. After incubation, we washed the well with 500 ul TBS before adding 100 ul Streptavidin (Rockland, #S000-01) diluted in TBS-BB (2 ug/ml final) to the well and incubated at room temperature for 5 min. After washing again with 500 ul TBS-BB, we added LOV2 diluted in TBS-BB (typically between 20–200 nM) to the well and incubated in the dark at 37C for 5 min. We then flushed the well with 500 ul HBSS-BB and incubated with cells previously labeled with the halo dye washed into HBSS-BB-FBS. Cells adhered to the SLB in the dark for 5 min at 37C before imaging on the microscope.

Buffers for SLB functionalization and imaging

- TBS: 150mM NaCl, 20mM Tris Base, pH 7.5
- TBS-BB: TBS with 2 mg/ml BSA and 0.5 mM β ME.
- mHBSS: 150mM NaCl, 40mM KCl, 1mM CaCl₂, 2mM MgCl₂, 10mM Glucose, 20mM HEPES, pH 7.2
- mHBSS-BB: mHBSS with 2 mg/ml BSA and 0.5 mM β ME

- Imaging media: mHBSS-BB supplemented with 2% fetal bovine serum, 50 ug/ml ascorbic acid and 1:100 dilution of ProLong Live Antifade Reagent (ThermoFisher Scientific, #P36975). Solution incubated at room temperature for at least 90 min to allow the antifade reagent to reduce oxygen levels.

Microscopy

Imaging was performed on an Eclipse Ti inverted microscope (Nikon) with two tiers of dichroic turrets to allow simultaneous fluorescence imaging and optogenetic stimulation. The microscope was also equipped with a motorized laser TIRF illumination unit, 60x and 100x Apochromat TIRF 1.49 NA objective (Nikon), an iXon Ultra EMCCD camera (Andor), and a laser launch (Versalase, Vortran) equipped with 405-, 488-, 561-, and 640 nm laser lines. For RICM, light from a Xenon arc lamp (Lambda LS, Sutter Instrument) source was passed through a 572/35 nm excitation filter (Chroma, #ET572/35x) filter and then a 50/50 beam splitter (Chroma, #21000). Microscope and associated hardware was controlled with MicroManager (Edelstein et al., 2014) in combination with custom built Arduino controllers (Advanced Research Consulting Corporation). Blue light for optogenetic stimulation was from a 470 nm LED (Lightspeed Technologies Inc., #HPLS-36), controlled with custom micromanager scripts. For most timepoints, only RICM and TIRF561 images were collected. During and in between these timepoints, a TIRF488 long-pass dichroic mirror remained permanently in the top dichroic turret, ensuring the blue-light illumination of the cells was never interrupted. The top TIRF488 dichroic passed the longer wavelengths used for RICM and TIRF561. Only when LOV2 localization was imaged with TIRF488 at the end of a three-minute

stimulation was the top dichroic removed to allow the shorter fluorescence excitation light to pass.

Image processing

After each day of imaging, we captured TIRF488, TIRF561 and RICM images of slides with concentrated solutions of fluorescein, Rose Bengal or dPBS, respectively. To flat field correct, we subtracted the camera offset from both the experimental and dye images. By dividing the experimental image by the median dye slide image, we acquired the final flat field corrected image used in analysis (Model, 2006).

Time course overview

We exposed cells to five minute blocks of constant blue light stimulation. Each block consisted of an initial two minute hold in strong blue light followed by a three minute stimulation at a fixed intensity of intermediate blue light. To measure the reporter output we averaged the final four timeframes of each condition. We measured CAR occupancy from a long exposure TIRF488 image taken at the end of the three minute stimulation, after the last biosensor output measurement made in TIRF561. As fluorescence excitation light from TIRF488 potentially stimulates LOV2, the TIRF488 channel could only be imaged once at the very end of a three minute stimulation. We repeated five minute blocks over the course of an hour experiment with a variety of blue light intensities to sample different ligand-binding half-lives.

CAR Occupancy Measurements

We background subtracted and background subtracted and thresholded RICM images at each timeframe to create a mask of cell footprints. The thresholded image was labeled using python skimage watershed algorithm (Van der Walt et al., 2014). A second local background mask was made by labeling pixels surrounding an expanded perimeter of each labeled cell in the cell mask. At steady state, free LOV2 should be homogeneously distributed on the SLB. The mean TIRF488 pixel intensity of a cell footprint is the sum of free LOV2 and LOV2 bound to the CAR. The mean TIRF488 pixel intensity in the background mask reflects free LOV2. Therefore, we calculated CAR occupancy as the mean TIRF488 pixel intensity in the cell mask minus the mean TIRF488 pixel intensity in the background mask.

Biosensor measurements

To calculate biosensor output levels at steady state, we averaged the TIRF561 pixel intensity within each labeled cell mask over the last four timeframes (equivalent to the last 40s) of a three-minute hold in blue light. To account for differences in biosensor expression level, we normalized cells to their average biosensor intensity in the absence of signaling (taken as the average of the last two TIRF561 images of each two minute reset pulse of intense blue light). We sometimes observed drift in a cell's basal activity over time. To correct for this drift, we subtracted the mean TIRF561 pixel intensity of each preceding two minute reset pulse of intense blue light from the mean value of the proceeding three-minute stimulation of blue light. Thus the reported

biosensor output value is the fold-change from the cell's average basal activity minus the fold-change from resented basal activity

Prior to model fitting, the biosensor output values of a biological replicate dataset (consisting of multiple wells acquired on the same day) were normalized by the 90th percentile output value in the dataset to properly normalize the data to the model, and to allow comparison between biosensors of variable dynamic ranges.

Criteria for including or excluding cells in analysis

We only analyzed cells present for the full time course. Cells that detached partway through the time course or arrived after the experiment began were excluded. Each replicate began with a no-light (maximal half-life) condition to identify non-responding cells. Cells that did not exhibit at least a 10% increase in reporter output above their basal output were excluded from analysis.

Biological and technical replicates

A biological replicate consisted of two time courses of stimulating cells with blue light on SLBs with different concentrations of LOV2, all on the same day (to ensure the light path did not change). We conducted each biological replicate on different days, with new preparations of cells, SLBs and LOV2. Each time course within a biological replicate contained approximately 30 cells, whose biosensor output levels and receptor occupancy were measured in all half-life conditions. As the microscopy experiments

could not be done in parallel and each biological replicate took an entire day, We could not conduct technical replicates.

LOV2 binding half-life measurements

We calculated the average Zdk binding half-life for each blue light condition as described previously (Tischer & Weiner, 2019)/

Kinetic proofreading model fitting

We fit each biological replicate dataset to the simple model of kinetic proofreading described previously (**Fig 3D**) (Tischer & Weiner, 2019). We fit each dataset using non-linear least-squares regression as implemented by the `curve_fit` function from the SciPy library (Virtanen et al., 2020).

References

- Andreotti, A. H., Schwartzberg, P. L., Joseph, R. E., & Berg, L. J. (2010). T-Cell Signaling Regulated by the Tec Family Kinase, Itk. *Cold Spring Harbor Perspectives in Biology*, 2(7), a002287.
<https://doi.org/10.1101/cshperspect.a002287>
- Balagopalan, L., Kortum, R. L., Coussens, N. P., Barr, V. A., & Samelson, L. E. (2015). The Linker for Activation of T Cells (LAT) Signaling Hub: From Signaling Complexes to Microclusters *. *Journal of Biological Chemistry*, 290(44), 26422–26429. <https://doi.org/10.1074/jbc.R115.665869>
- Bhardwaj, N., Young, J. W., Nisanian, A. J., Baggers, J., & Steinman, R. M. (1993). Small amounts of superantigen, when presented on dendritic cells, are sufficient to initiate T cell responses. *Journal of Experimental Medicine*, 178(2), 633–642.
<https://doi.org/10.1084/jem.178.2.633>
- Bhatia, S., Edidin, M., Almo, S. C., & Nathenson, S. G. (2005). Different cell surface oligomeric states of B7-1 and B7-2: Implications for signaling. *Proceedings of the National Academy of Sciences*, 102(43), 15569–15574.
<https://doi.org/10.1073/pnas.0507257102>
- Borroto, A., Arellano, I., Blanco, R., Fuentes, M., Orfao, A., Dopfer, E. P., Prouza, M., Suchànek, M., Schamel, W. W., & Alarcón, B. (2014). Relevance of Nck–CD3ε Interaction for T Cell Activation In Vivo. *The Journal of Immunology*, 192(5), 2042–2053. <https://doi.org/10.4049/jimmunol.1203414>
- Bromley, S. K., & Dustin, M. L. (2002). Stimulation of naïve T-cell adhesion and immunological synapse formation by chemokine-dependent and -independent

mechanisms. *Immunology*, 106(3), 289–298. <https://doi.org/10.1046/j.1365-2567.2002.01441.x>

Burgess, S. M., & Guthrie, C. (1993). A mechanism to enhance mRNA splicing fidelity: The RNA-dependent ATPase Prp16 governs usage of a discard pathway for aberrant lariat intermediates. *Cell*, 73(7), 1377–1391.
[https://doi.org/10.1016/0092-8674\(93\)90363-u](https://doi.org/10.1016/0092-8674(93)90363-u)

Cameron, B. J., Gerry, A. B., Dukes, J., Harper, J. V., Kannan, V., Bianchi, F. C., Grand, F., Brewer, J. E., Gupta, M., Plesa, G., Bossi, G., Vuidepot, A., Powlesland, A. S., Legg, A., Adams, K. J., Bennett, A. D., Pumphrey, N. J., Williams, D. D., Binder-Scholl, G., ... Jakobsen, B. K. (2013). Identification of a Titin-Derived HLA-A1–Presented Peptide as a Cross-Reactive Target for Engineered MAGE A3–Directed T Cells. *Science Translational Medicine*, 5(197), 197ra103-197ra103. <https://doi.org/10.1126/scitranslmed.3006034>

Chakraborty, A. K., & Weiss, A. (2014). Insights into the initiation of TCR signaling. *Nature Immunology*, 15(9), 798–807. <https://doi.org/10.1038/ni.2940>

Christinck, E. R., Luscher, M. A., Barber, B. H., & Williams, D. B. (1991). Peptide binding to class I MHC on living cells and quantitation of complexes required for CTL lysis. *Nature*, 352(6330), 67–70. <https://doi.org/10.1038/352067a0>

Cohen, C. J., Sarig, O., Yamano, Y., Tomaru, U., Jacobson, S., & Reiter, Y. (2003). Direct Phenotypic Analysis of Human MHC Class I Antigen Presentation: Visualization, Quantitation, and In Situ Detection of Human Viral Epitopes Using Peptide-Specific, MHC-Restricted Human Recombinant Antibodies. *The Journal of Immunology*, 170(8), 4349–4361. <https://doi.org/10.4049/jimmunol.170.8.4349>

- Coombs, D., & Goldstein, B. (2005). T cell activation: Kinetic proofreading, serial engagement and cell adhesion. *Journal of Computational and Applied Mathematics*, 184(1), 121–139. <https://doi.org/10.1016/j.cam.2004.07.035>
- Courtney, A. H., Lo, W.-L., & Weiss, A. (2018). TCR SIGNALING: MECHANISMS OF INITIATION AND PROPAGATION. *Trends in Biochemical Sciences*, 43(2), 108–123. <https://doi.org/10.1016/j.tibs.2017.11.008>
- Daniels, M. A., Teixeira, E., Gill, J., Hausmann, B., Roubaty, D., Holmberg, K., Werlen, G., Holländer, G. A., Gascoigne, N. R. J., & Palmer, E. (2006). Thymic selection threshold defined by compartmentalization of Ras/MAPK signalling. *Nature*, 444(7120), 724–729. <https://doi.org/10.1038/nature05269>
- Davis, M. M., Boniface, J. J., Reich, Z., Lyons, D., Hampl, J., Arden, B., & Chien, Y. (1998). LIGAND RECOGNITION BY $\alpha\beta$ T CELL RECEPTORS. *Annual Review of Immunology*, 16(1), 523–544. <https://doi.org/10.1146/annurev.immunol.16.1.523>
- Davis, S. J., & van der Merwe, P. A. (2006). The kinetic-segregation model: TCR triggering and beyond. *Nature Immunology*, 7(8), 803–809. <https://doi.org/10.1038/ni1369>
- Deindl, S., Kadlecsek, T. A., Cao, X., Kuriyan, J., & Weiss, A. (2009). Stability of an autoinhibitory interface in the structure of the tyrosine kinase ZAP-70 impacts T cell receptor response. *Proceedings of the National Academy of Sciences*, 106(49), 20699–20704. <https://doi.org/10.1073/pnas.0911512106>
- Demotz, S., Grey, H. M., & Sette, A. (1990). The minimal number of class II MHC-antigen complexes needed for T cell activation. *Science*, 249(4972), 1028–1030.

<https://doi.org/10.1126/science.2118680>

Dustin, M. L., Starr, T., Varma, R., & Thomas, V. K. (2007). Supported Planar Bilayers for Study of the Immunological Synapse. *Current Protocols in Immunology*, 76(1), 18.13.1-18.13.35. <https://doi.org/10.1002/0471142735.im1813s76>

Edelstein, A. D., Tsuchida, M. A., Amodaj, N., Pinkard, H., Vale, R. D., & Stuurman, N. (2014). Advanced methods of microscope control using μ Manager software. *Journal of Biological Methods*, 1(2), e10–e10. <https://doi.org/10.14440/jbm.2014.36>

Gascoigne, N. R. J., Zal, T., & Alam, S. M. (2001). T-cell receptor binding kinetics in T-cell development and activation. *Expert Reviews in Molecular Medicine*, 3(6), 1–17. <https://doi.org/10.1017/S1462399401002502>

Germain, R. N., & Stefanová, I. (1999). THE DYNAMICS OF T CELL RECEPTOR SIGNALING: Complex Orchestration and the Key Roles of Tempo and Cooperation. *Annual Review of Immunology*, 17(1), 467–522. <https://doi.org/10.1146/annurev.immunol.17.1.467>

Goyette, J., Depoil, D., Yang, Z., Isaacson, S. A., Allard, J., Merwe, P. A. van der, Gaus, K., Dustin, M. L., & Dushek, O. (2020). *Regulated unbinding of ZAP70 at the T cell receptor by kinetic avidity* (p. 2020.02.12.945170). <https://doi.org/10.1101/2020.02.12.945170>

Grimm, J. B., English, B. P., Chen, J., Slaughter, J. P., Zhang, Z., Revyakin, A., Patel, R., Macklin, J. J., Normanno, D., Singer, R. H., Lionnet, T., & Lavis, L. D. (2015). A general method to improve fluorophores for live-cell and single-molecule microscopy. *Nature Methods*, 12(3), 244–250.

<https://doi.org/10.1038/nmeth.3256>

Hopfield, J. J. (1974). Kinetic Proofreading: A New Mechanism for Reducing Errors in Biosynthetic Processes Requiring High Specificity. *Proceedings of the National Academy of Sciences*, 71(10), 4135–4139.

<https://doi.org/10.1073/pnas.71.10.4135>

Hsu, L.-Y., Cheng, D. A., Chen, Y., Liang, H.-E., & Weiss, A. (2017). Destabilizing the autoinhibitory conformation of Zap70 induces up-regulation of inhibitory receptors and T cell unresponsiveness. *The Journal of Experimental Medicine*, 214(3), 833–849. <https://doi.org/10.1084/jem.20161575>

Huang, W. Y. C., Alvarez, S., Kondo, Y., Lee, Y. K., Chung, J. K., Lam, H. Y. M., Biswas, K. H., Kuriyan, J., & Groves, J. T. (2019). A molecular assembly phase transition and kinetic proofreading modulate Ras activation by SOS. *Science*, 363(6431), 1098–1103. <https://doi.org/10.1126/science.aau5721>

Huse, M., Klein, L. O., Girvin, A. T., Faraj, J. M., Li, Q.-J., Kuhns, M. S., & Davis, M. M. (2007). Spatial and Temporal Dynamics of T Cell Receptor Signaling with a Photoactivatable Agonist. *Immunity*, 27(1), 76–88. <https://doi.org/10.1016/j.immuni.2007.05.017>

Irvine, D. J., Purbhoo, M. A., Krogsaard, M., & Davis, M. M. (2002). Direct observation of ligand recognition by T cells. *Nature*, 419(6909), 845–849. <https://doi.org/10.1038/nature01076>

Irving, B. A., & Weiss, A. (1991). The cytoplasmic domain of the T cell receptor ζ chain is sufficient to couple to receptor-associated signal transduction pathways. *Cell*, 64(5), 891–901. [https://doi.org/10.1016/0092-8674\(91\)90314-O](https://doi.org/10.1016/0092-8674(91)90314-O)

James, J. R., & Vale, R. D. (2012). Biophysical mechanism of T-cell receptor triggering in a reconstituted system. *Nature*, *487*(7405), 64–69.

<https://doi.org/10.1038/nature11220>

Kim, S. T., Takeuchi, K., Sun, Z.-Y. J., Touma, M., Castro, C. E., Fahmy, A., Lang, M.

J., Wagner, G., & Reinherz, E. L. (2009). The $\alpha\beta$ T Cell Receptor Is an Anisotropic Mechanosensor *. *Journal of Biological Chemistry*, *284*(45), 31028–

31037. <https://doi.org/10.1074/jbc.M109.052712>

Kim, S. T., Touma, M., Takeuchi, K., Sun, Z.-Y. J., Dave, V. P., Kappes, D. J., Wagner,

G., & Reinherz, E. L. (2010). Distinctive CD3 Heterodimeric Ectodomain

Topologies Maximize Antigen-Triggered Activation of $\alpha\beta$ T Cell Receptors. *The Journal of Immunology*, *185*(5), 2951–2959.

<https://doi.org/10.4049/jimmunol.1000732>

Kimachi, K., Croft, M., & Grey, H. M. (1997). The minimal number of antigen-major histocompatibility complex class II complexes required for activation of naive and primed T cells. *European Journal of Immunology*, *27*(12), 3310–3317.

<https://doi.org/10.1002/eji.1830271230>

Korem Kohanim, Y., Tendler, A., Mayo, A., Friedman, N., & Alon, U. (2020). Endocrine

Autoimmune Disease as a Fragility of Immune Surveillance against Hypersecreting Mutants. *Immunity*, *52*(5), 872-884.e5.

<https://doi.org/10.1016/j.immuni.2020.04.022>

Labadia, M. E., Jeanfavre, D. D., Caviness, G. O., & Morelock, M. M. (1998). Molecular

Regulation of the Interaction Between Leukocyte Function-Associated Antigen-1 and Soluble ICAM-1 by Divalent Metal Cations. *The Journal of Immunology*,

161(2), 836–842.

- Lin, J. J. Y., Low-Nam, S. T., Alfieri, K. N., McAfee, D. B., Fay, N. C., & Groves, J. T. (2019). Mapping the stochastic sequence of individual ligand-receptor binding events to cellular activation: T cells act on the rare events. *Science Signaling*, 12(564), eaat8715. <https://doi.org/10.1126/scisignal.aat8715>
- Lo, W.-L., Shah, N. H., Rubin, S. A., Zhang, W., Horkova, V., Fallahee, I. R., Stepanek, O., Zon, L. I., Kuriyan, J., & Weiss, A. (2019). Slow phosphorylation of a tyrosine residue in LAT optimizes T cell ligand discrimination. *Nature Immunology*, 20(11), 1481–1493. <https://doi.org/10.1038/s41590-019-0502-2>
- Manz, B. N., Jackson, B. L., Petit, R. S., Dustin, M. L., & Groves, J. (2011). T-cell triggering thresholds are modulated by the number of antigen within individual T-cell receptor clusters. *Proceedings of the National Academy of Sciences*. <https://doi.org/10.1073/pnas.1018771108>
- McKeithan, T. W. (1995). Kinetic proofreading in T-cell receptor signal transduction. *Proceedings of the National Academy of Sciences*, 92(11), 5042–5046. <https://doi.org/10.1073/pnas.92.11.5042>
- Model, M. A. (2006). Intensity calibration and shading correction for fluorescence microscopes. *Current Protocols in Cytometry, Chapter 10*, Unit10.14. <https://doi.org/10.1002/0471142956.cy1014s37>
- Ninio, J. (1975). Kinetic amplification of enzyme discrimination. *Biochimie*, 57(5), 587–595. [https://doi.org/10.1016/S0300-9084\(75\)80139-8](https://doi.org/10.1016/S0300-9084(75)80139-8)
- Nye, J. A., & Groves, J. T. (2008). Kinetic Control of Histidine-Tagged Protein Surface Density on Supported Lipid Bilayers. *Langmuir*, 24(8), 4145–4149.

<https://doi.org/10.1021/la703788h>

O'Donoghue, G. P., Pielak, R. M., Smoligovets, A. A., Lin, J. J., & Groves, J. T. (2013).

Direct single molecule measurement of TCR triggering by agonist pMHC in living primary T cells. *ELife*, 2, e00778. <https://doi.org/10.7554/eLife.00778>

Pettmann, J., Huhn, A., Abu Shah, E., Kutuzov, M. A., Wilson, D. B., Dustin, M. L.,

Davis, S. J., van der Merwe, P. A., & Dushek, O. (2021). The discriminatory power of the T cell receptor. *ELife*, 10, e67092.

<https://doi.org/10.7554/eLife.67092>

Razvag, Y., Neve-Oz, Y., Sajman, J., Reches, M., & Sherman, E. (2018). Nanoscale

kinetic segregation of TCR and CD45 in engaged microvilli facilitates early T cell activation. *Nature Communications*, 9(1), 732. [https://doi.org/10.1038/s41467-](https://doi.org/10.1038/s41467-018-03127-w)

[018-03127-w](https://doi.org/10.1038/s41467-018-03127-w)

Schoenborn, J. R., Tan, Y. X., Zhang, C., Shokat, K. M., & Weiss, A. (2011). Feedback

Circuits Monitor and Adjust Basal Lck-Dependent Events in T Cell Receptor Signaling. *Science Signaling*, 4(190), ra59–ra59.

<https://doi.org/10.1126/scisignal.2001893>

Shen, L., Matloubian, M., Kadlecsek, T. A., & Weiss, A. (2021). A disease-associated

mutation that weakens ZAP70 autoinhibition enhances responses to weak and self-ligands. *Science Signaling*, 14(668).

<https://doi.org/10.1126/scisignal.abc4479>

Sherman, E., Barr, V., Manley, S., Patterson, G., Balagopalan, L., Akpan, I., Regan, C.

K., Merrill, R. K., Sommers, C. L., Lippincott-Schwartz, J., & Samelson, L. E.

(2011). Functional Nanoscale Organization of Signaling Molecules Downstream

- of the T Cell Antigen Receptor. *Immunity*, 35(5), 705–720.
<https://doi.org/10.1016/j.immuni.2011.10.004>
- Springer, T. A. (1990). Adhesion receptors of the immune system. *Nature*, 346(6283), 425–434. <https://doi.org/10.1038/346425a0>
- Stepanek, O., Prabhakar, A. S., Osswald, C., King, C. G., Bulek, A., Naeher, D., Beaufile-Hugot, M., Abanto, M. L., Galati, V., Hausmann, B., Lang, R., Cole, D. K., Huseby, E. S., Sewell, A. K., Chakraborty, A. K., & Palmer, E. (2014). Co-receptor scanning by the T-cell receptor provides a mechanism for T cell tolerance. *Cell*, 159(2), 333–345. <https://doi.org/10.1016/j.cell.2014.08.042>
- Su, X., Ditlev, J. A., Hui, E., Xing, W., Banjade, S., Okrut, J., King, D. S., Taunton, J., Rosen, M. K., & Vale, R. D. (2016). Phase separation of signaling molecules promotes T cell receptor signal transduction. *Science*, 352(6285), 595–599. <https://doi.org/10.1126/science.aad9964>
- Sykulev, Y., Joo, M., Vturina, I., Tsomides, T. J., & Eisen, H. N. (1996). Evidence that a Single Peptide–MHC Complex on a Target Cell Can Elicit a Cytolytic T Cell Response. *Immunity*, 4(6), 565–571. [https://doi.org/10.1016/S1074-7613\(00\)80483-5](https://doi.org/10.1016/S1074-7613(00)80483-5)
- Tan, Y. X., Manz, B. N., Freedman, T. S., Zhang, C., Shokat, K. M., & Weiss, A. (2014). Inhibition of the kinase Csk in thymocytes reveals a requirement for actin remodeling in the initiation of full TCR signaling. *Nature Immunology*, 15(2), 186–194. <https://doi.org/10.1038/ni.2772>
- Tischer, D. K., & Weiner, O. D. (2019). Light-based tuning of ligand half-life supports kinetic proofreading model of T cell signaling. *ELife*, 8, e42498.

<https://doi.org/10.7554/eLife.42498>

- Unternaehrer, J. J., Chow, A., Pypaert, M., Inaba, K., & Mellman, I. (2007). The tetraspanin CD9 mediates lateral association of MHC class II molecules on the dendritic cell surface. *Proceedings of the National Academy of Sciences*, *104*(1), 234–239. <https://doi.org/10.1073/pnas.0609665104>
- Van der Walt, S., Schönberger, J. L., Nunez-Iglesias, J., Boulogne, F., Warner, J. D., Yager, N., Gouillart, E., & Yu, T. (2014). scikit-image: Image processing in Python. *PeerJ*, *2*, e453.
- Virtanen, P., Gommers, R., Oliphant, T. E., Haberland, M., Reddy, T., Cournapeau, D., Burovski, E., Peterson, P., Weckesser, W., Bright, J., van der Walt, S. J., Brett, M., Wilson, J., Millman, K. J., Mayorov, N., Nelson, A. R. J., Jones, E., Kern, R., Larson, E., ... SciPy 1.0 Contributors. (2020). SciPy 1.0: Fundamental Algorithms for Scientific Computing in Python. *Nature Methods*, *17*, 261–272. <https://doi.org/10.1038/s41592-019-0686-2>
- Wang, J., Jelcic, I., Mühlenbruch, L., Hauerndinger, V., Toussaint, N. C., Zhao, Y., Cruciani, C., Faigle, W., Naghavian, R., Foege, M., Binder, T. M. C., Eiermann, T., Opitz, L., Fuentes-Font, L., Reynolds, R., Kwok, W. W., Nguyen, J. T., Lee, J.-H., Lutterotti, A., ... Martin, R. (2020). HLA-DR15 Molecules Jointly Shape an Autoreactive T Cell Repertoire in Multiple Sclerosis. *Cell*, *183*(5), 1264-1281.e20. <https://doi.org/10.1016/j.cell.2020.09.054>
- Yao, X., Rosen, M. K., & Gardner, K. H. (2008). Estimation of Available Free Energy in a LOV2- α Photoswitch. *Nature Chemical Biology*, *4*(8), 491–497. <https://doi.org/10.1038/nchembio.99>

- Yi, J., Balagopalan, L., Nguyen, T., McIntire, K. M., & Samelson, L. E. (2019). TCR microclusters form spatially segregated domains and sequentially assemble in calcium-dependent kinetic steps. *Nature Communications*, *10*(1), 277.
<https://doi.org/10.1038/s41467-018-08064-2>
- Yin, Y., Li, Y., & Mariuzza, R. A. (2012). Structural basis for self-recognition by autoimmune T-cell receptors. *Immunological Reviews*, *250*(1), 32–48.
<https://doi.org/10.1111/imr.12002>

Figure 1

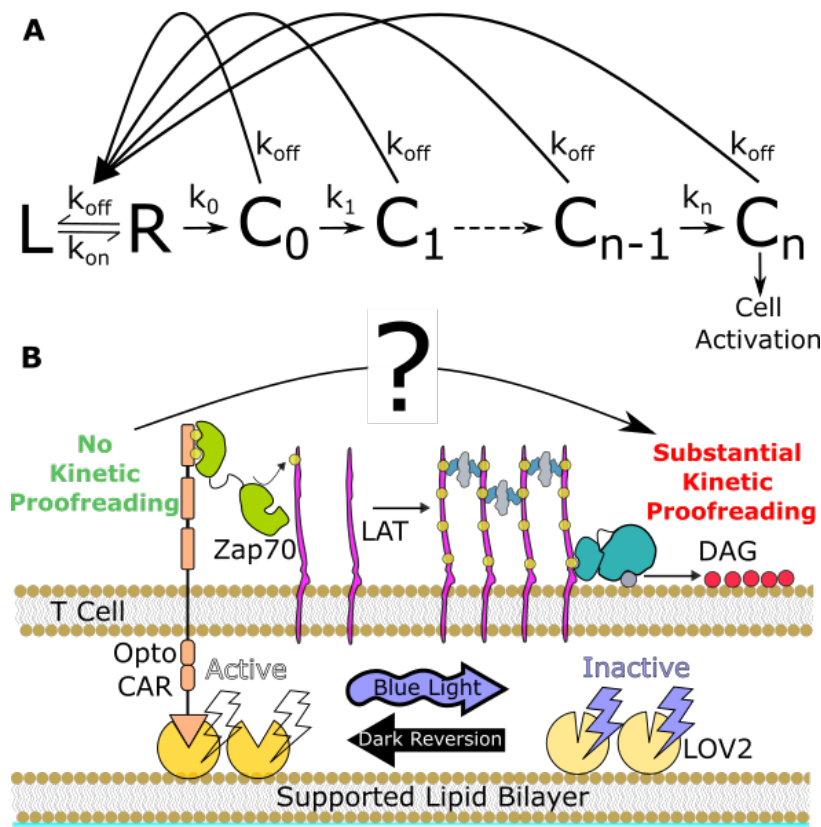


Figure 1 What steps of T cell activation generate kinetic proofreading behavior?

(A) The Kinetic Proofreading model consists of a chain of events that begin once the ligand (L) binds the receptor (R). If the ligand unbinds the receptor at any time all signaling intermediate (C_i) reset back to the ground state. Only binding events that last long enough to form the active terminal signaling complex (C_n) contribute to cell activation. All shorter binding events reset before C_n can form and are invisible to the cell. **(B)** Previous findings from our lab showed kinetic proofreading in DAG generation but none in ZAP70 recruitment. With our optogenetic system we can control ligand-receptor interactions with blue light. We use a supported lipid bilayer functionalized with the light-sensitive protein LOV2 to create an artificial antigen presenting surface. Jurkat cells expressing our optogenetic CAR bind to the LOV2 and activate antigen signaling. We measure live-cell signaling reporters also expressed in the Jurkat cells with TIRF microscopy while simultaneously manipulating the CAR-LOV2 interaction with blue light. The opto-CAR binds ground-state LOV2 with high affinity but binds excited LOV2 with extremely low affinity. Absorption of a photon instantly interrupts a LOV2-CAR binding event. With this system we can control the average binding lifetime with the flux of photons at the sample. Using this system we previously measured kinetic proofreading behavior in the generation of diacylglycerol, but measured no proofreading behavior in the recruitment of ZAP70. With this work we investigate where in proximal T cell antigen signaling the kinetic proofreading behavior of DAG generation arises.

Figure 2

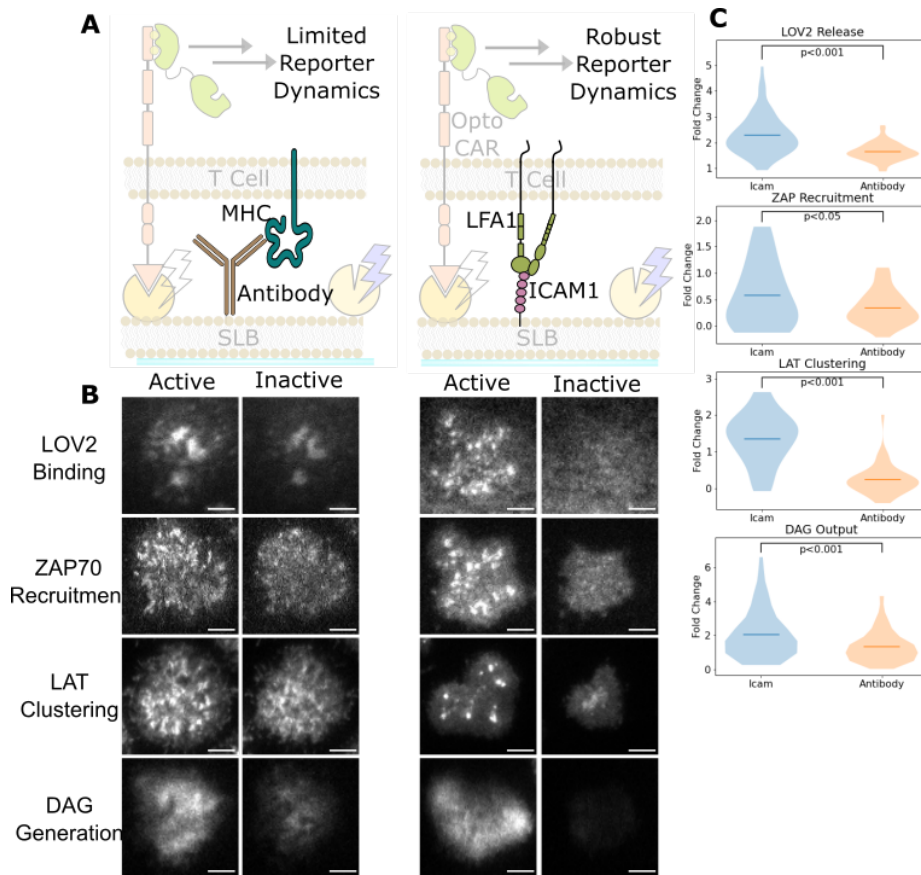


Figure 2 ICAM-1 adhesion improves biosensor robustness

(A) In our previous work we adhered cells SLB through biotinylated beta2 microglobulin antibodies against the cells' MHC class1 functionalized to biotin-streptavidin capped lipids in the SLB (left). This adhesion technique enabled adequate DAG biosensor dynamics, but limited the spatiotemporal dynamics of many other biosensors, including the recruitment of ZAP70 and the clustering of LAT. For this work, cells adhere to the bilayer through native LFA-1 integrin signaling via ICAM-1-HIS functionalized to Ni-NTA capped lipids in the SLB (right). **(B)** Representative TIF Images of LOV2 binding, Zap70 recruitment, LAT clustering, and DAG generation changes after two minutes of strong inactivation of the Zdk-CAR under antibody adhesion (left), and ICAM-1 adhesion (right) (scale bar = 5um). SLB adhesion through ICAM-1-HIS improved the spatiotemporal dynamics. **(C)** Quantification of the fold change in LOV2 binding, Zap70 recruitment, LAT clustering, and DAG generation between active and inactive Zdk-CAR signaling states under ICAM-1 adhesion (left) and antibody adhesion (right). The max pixel intensity per cell under active signaling (no-light) was normalized to the subsequent max pixel value after 2 minutes of inactive signaling (intense light) (independent t-test p values shown).

Figure 3

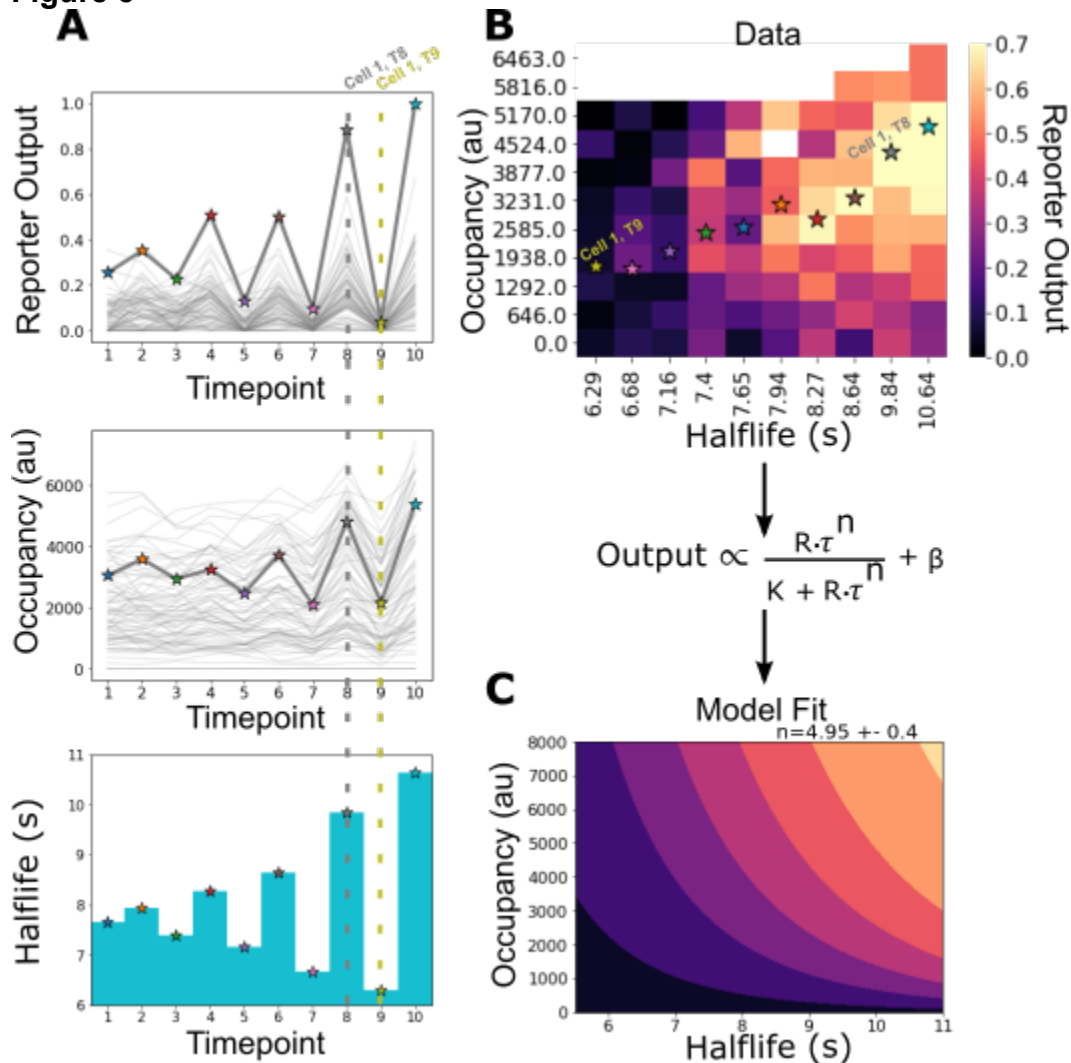


Figure 3 Optogenetic timecourse and model fitting overview

(A) After adhering the cells to the functionalized SLBs we expose them to a series of three minutes blue-light conditions with known average ligand binding half-lives. At the end of each half-life condition we measure every cell's steady-state reporter output and receptor occupancy (arbitrary cell highlighted at time point 8 and 9 as example). Following this protocol we measure every cell's reporter output as a function of receptor occupancy and average ligand binding half-life. **(B)** After normalizing each cell to its average basal reporter activity, the data from multiple time courses are aggregated and the reporter output values are normalized to the 90th percentile cell in the dataset. **(C)** The dataset is then fit to a simple model of the expected output of a kinetic proofreading signaling system. In the model the expected signaling output is proportional to the ligand occupancy (R) and ligand binding half-life (τ) raised to the number of strong proofreading steps (n) upstream of that signaling step. The magnitude of n provides a relative value of the strength of kinetic proofreading between that events and ligand binding.

Figure 4

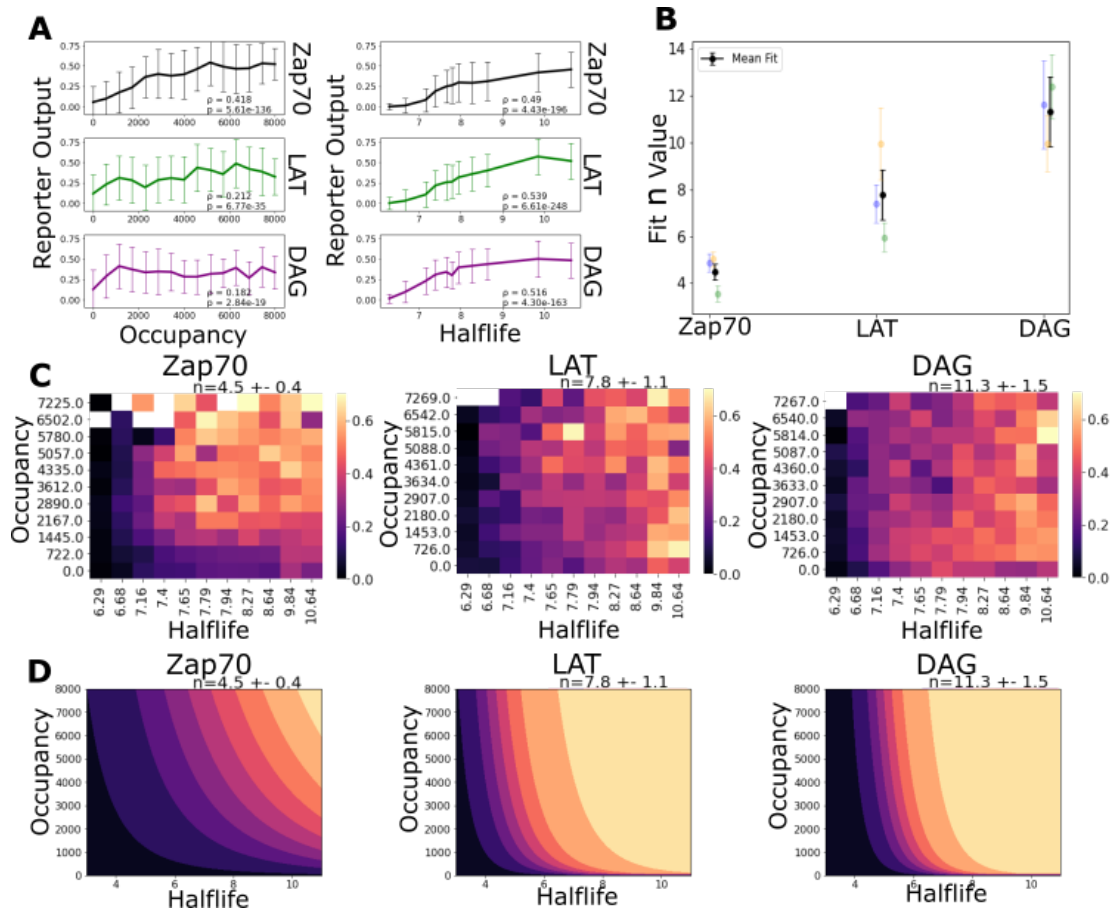


Figure 4 Kinetic proofreading starts at receptor activation and increases in strength at terminal signaling complexes

(A) The reporter output of Zap70 recruitment, LAT clustering, and DAG generation plotted as a function of receptor occupancy (left) and average ligand binding half-life (right). Zap70 recruitment correlated the most with receptor occupancy (spearman $\rho = 0.42$) while DAG generation correlated the least ($\rho = 0.18$). All biosensors showed strong correlation with ligand binding half-life ($\rho \sim 0.5$). **(B)** The fit n-values (+/- 1 std) for each biosensor across three biological replicates with the mean n-value fit plotted in black. The fit n-values continued to increase from Zap70 recruitment to LAT cluster to DAG generation. These results suggest the existence of kinetic proofreading steps between ligand-binding and Zap70 recruitment, between the recruitment of Zap70 and the formation of a LAT cluster, and between the initial formation of a LAT cluster and the generation of DAG/IP3 from that cluster. **(C)** Heatmaps for each biosensor's aggregated data with biosensor output (color) plotted as a function of both occupancy (y-axis) and ligand binding half-life (x-axis). The mean fit n-values for each biosensor (+/- 1 std) is noted above the heatmap. **(D)** The expected model output for each biosensor using the mean fit values of the above datasets.

Figure 5

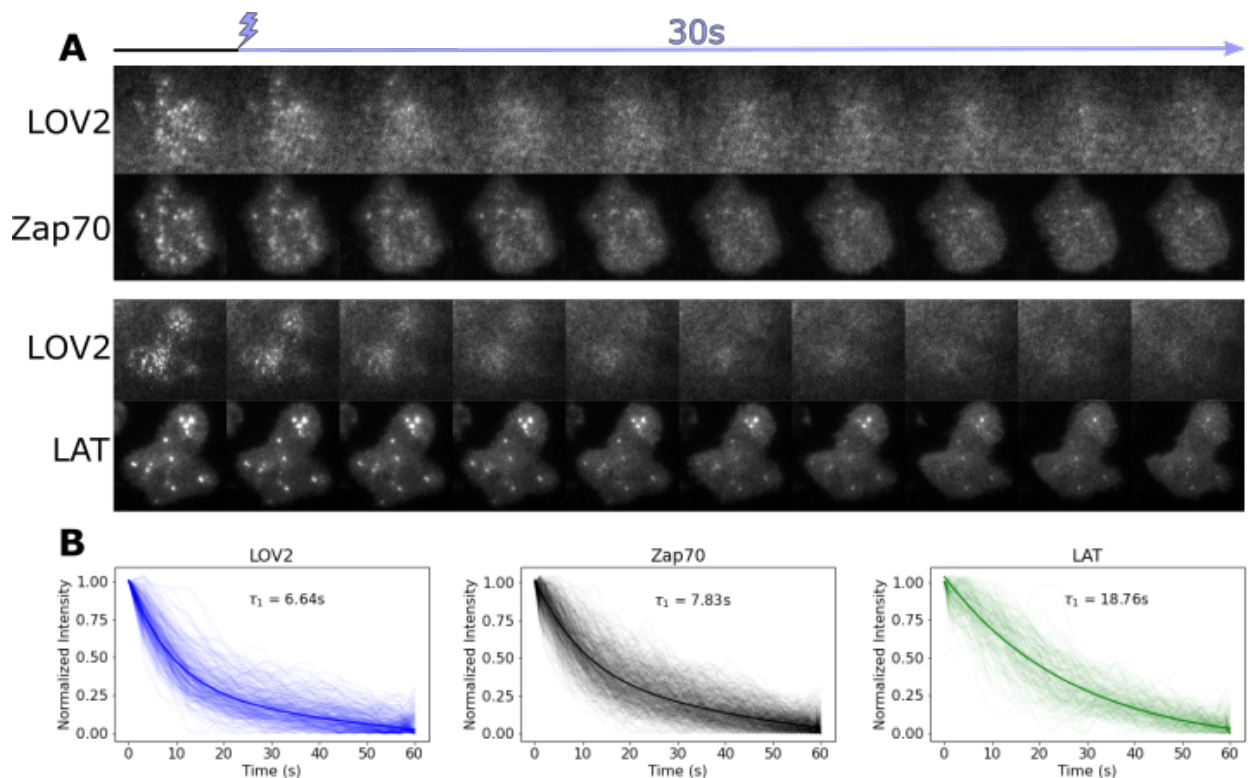
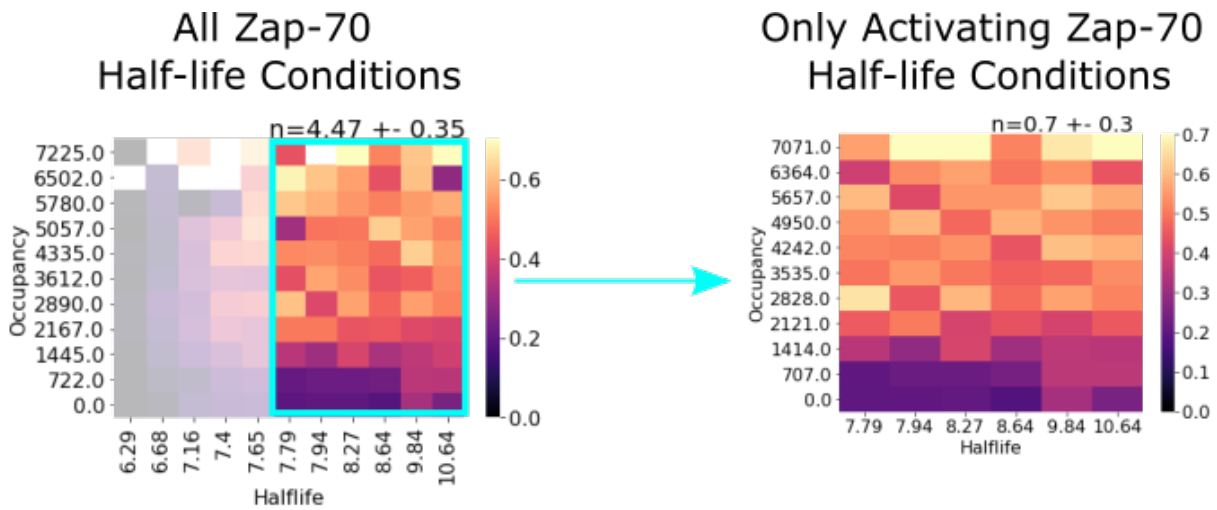


Fig 5 Terminal signaling complexes reset slower than active receptors upon ligand unbinding.

(A) Cells expressing either Zap70-Halo or LAT-Halo were allowed to activate for 3 minutes before acute inactivation with intense blue light for one minute. Subcellular clusters of LOV2, Zap70, and LAT were manually segmented and measured through time using ImageJ. Representative cells of Zap70 and LAT up signal inhibition with respective LOV2 images. **(B)** The resulting off-rate curves were fitted with bi-exponentials, which resulted in a short decay constant (reported) and a much longer constant likely due to photofluor bleaching or cell movement (**Fig S3**).

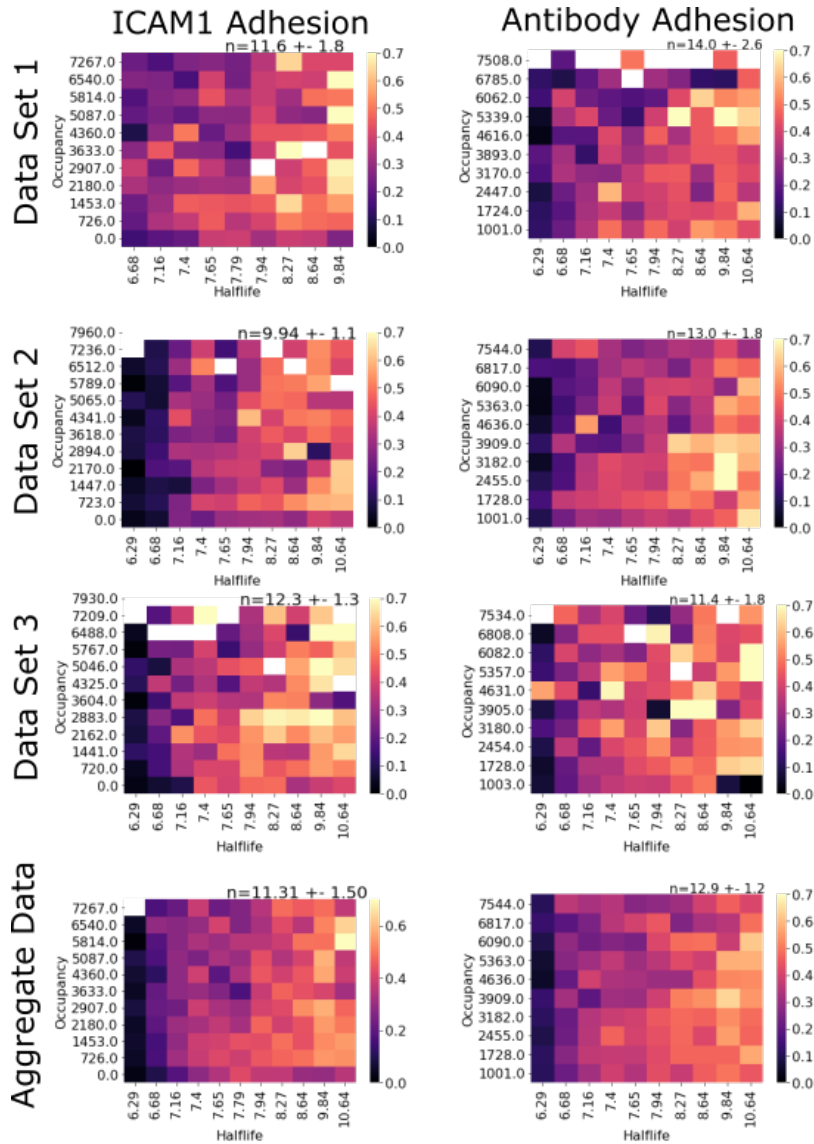
Figure S1



Supplementary Figure 1 Zap70 data subset recaptures previous reported value

In our previous work we measured no kinetic proofreading in Zap70 recruitment with supplementary bilayer adhesion. One potential explanation is without any bilayer adhesion, non-activated cells did not generate sufficient footprints for segmentation. If fit our model to only the activating half-life conditions of our current Zap70 dataset, we measure similarly low proofreading behavior ($n=0.7 \pm 0.3$).

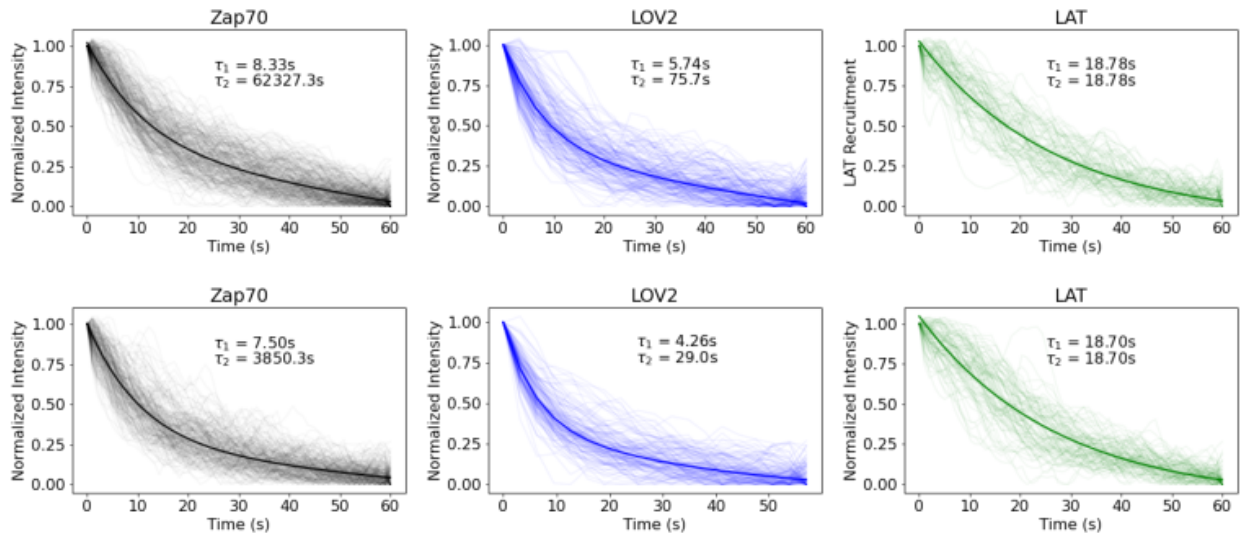
Figure S2



Supplementary Figure 2 Measured kinetic proofreading at DAG generation similar for ICAM-1 and antibody-based adhesion

Bilayer adhesion through ICAM-1 or antibody produces similar kinetic proofreading model fits for the generation of DAG. Biological replicates were conducted using antibody adhesion in place of ICAM-1 and analyzed in identical manner. Both adhesion methods fit strong proofreading to the generation of DAG.

Figure S3



Supplementary Figure 3 Replicate datasets for off-rate fits

Biological replicates of LOV2, Zap70, and LAT unbinding curve fit with bi-exponential functions. The fitted halflives are reported on each graph. Fits of LOV2 and Zap70 produced one halflife on the scale of the observed loss of the reporter, and a second much longer value likely a function of photobleaching or cellular movement. Both LAT replicates fit with identical halflife values, indicating mono-exponential data.

Publishing Agreement

It is the policy of the University to encourage open access and broad distribution of all theses, dissertations, and manuscripts. The Graduate Division will facilitate the distribution of UCSF theses, dissertations, and manuscripts to the UCSF Library for open access and distribution. UCSF will make such theses, dissertations, and manuscripts accessible to the public and will take reasonable steps to preserve these works in perpetuity.

I hereby grant the non-exclusive, perpetual right to The Regents of the University of California to reproduce, publicly display, distribute, preserve, and publish copies of my thesis, dissertation, or manuscript in any form or media, now existing or later derived, including access online for teaching, research, and public service purposes.

DocuSigned by:

Derek Britain

10756EA3AE624E5...

Author Signature

9/3/2021

Date